Comparative studies of various iron-mediated oxidative systems for the photochemical degradation of endosulfan in aqueous solution

Noor S. Shah [a,b,c], Xuexiang He [b,d], Javed Ali Khan [a,b], Hasan M. Khan [a], Dominic L. Boccelli [b], Dionysios D. Dionysiou [b,d],*

[a] Radiation Chemistry Laboratory, National Centre of Excellence in Physical Chemistry, University of Peshawar, Peshawar 25120, Pakistan
[b] Environmental Engineering and Science Program, University of Cincinnati, 705 Engineering Research Center, Cincinnati, OH 45221-0012, United States
[c] Institute of Chemical Sciences, University of Swat, Swat 19130, Pakistan
[d] Nireas-International Water Research Centre, University of Cyprus, Nicosia 1678, Cyprus

ABSTRACT

This study investigated iron-mediated oxidative processes for the photochemical degradation of endosulfan, a chlorinated insecticide and central nervous system disruptor. At UV fluence of $360 \, mJ/cm^2$, 52.4% and 32.0% removal of $2.45 \, \mu M$ initial endosulfan was observed by UV/Fe^{3+} and UV/Fe^{2+} processes, respectively, at an initial concentration of $17.8 \, \mu M$ iron. The degradation of endosulfan by UV/Fe^{3+} or UV/Fe^{2+} was dramatically enhanced by adding peroxide (i.e., H_2O_2, $S_2O_8^{2-}$ or HSO_5^-). Among the UV/peroxide/Fe processes, the highest degradation efficiency of 99.0% at UV fluence of $360 \, mJ/cm^2$ was observed by $UV/HSO_5^-/Fe^{2+}$ with $2.45 \, \mu M$ [endosulfan]$_0$, $17.8 \, \mu M$ [Fe^{2+}]$_0$, and $49.0 \, \mu M$ [HSO_5^-]$_0$. The observed degradation rate constant of endosulfan was promoted either by increasing [Fe^{2+}]$_0$ and/or [peroxide]$_0$ or by decreasing [endosulfan]$_0$, while the initial degradation rate of endosulfan increased with increasing [Fe^{2+}]$_0$, [peroxide]$_0$, or [endosulfan]$_0$. At UV fluence of $6000 \, mJ/cm^2$, 45.0% mineralization as represented by the decrease in total organic carbon content was observed by $UV/HSO_5^-/Fe^{2+}$ at $9.80 \, \mu M$ [endosulfan]$_0$, $980 \, \mu M$ [HSO_5^-]$_0$, and $17.8 \, \mu M$ [Fe^{2+}]$_0$. The major by-product of endosulfan was observed in all cases to be endosulfan ether which was further degraded with an extended reaction time. The results suggest that iron-mediated advanced oxidation processes (AOPs) have a high potential for the removal of endosulfan and its by-product from contaminated water.

1. Introduction

Organochlorine insecticides are an important class of pesticides, commonly used on wood, crops and vegetables for the control of mites, pests, and pest causing diseases [1]. However, many of them have been reported to be highly toxic and can affect the crop productivity [2], soil fertility [3], ecological balance [4], and human health [5]. One of the most known organochlorine insecticides is endosulfan (1,2,3,4,7,7-hexachlorobicyclo-2,2,1-heptene-2,3-bishydroxymethane-5,6-sulfite). It is commonly used on fruits, cotton, vegetables, tobacco, sugarcane, and tea for the control of tsetse fly, mites, home garden pests, Colorado potato beetles, and cabbage worms; it can also be used as a wood preservative [6,7]. The acute and chronic toxicity of endosulfan is widely recognized in a number of mammals including humans [8]. Moreover, endosulfan is non-volatile and is highly persistent in the environment, with a long half-life ranging from several months to several years [9,10]. Residues of endosulfan have therefore been detected in various environmental matrices such as water [11]. Considering its health risk, the US Environmental Protection Agency has classified endosulfan as a "priority pollutant (category Ib)" [12]. However, no control guidelines have been proposed for this emerging organic pollutant [13]. It is thus highly important to develop effective technologies for the detoxification of water contaminated with endosulfan.

Advanced oxidation processes (AOPs) are innovative treatment technologies that rely on in situ generation of reactive hydroxyl radical ($^\bullet OH$) [14]. Various AOPs have been developed and studied including Fenton (Fe^{2+}/H_2O_2) and Fenton-like (e.g., Fe^{3+}/H_2O_2) reactions, photo-Fenton ($UV/H_2O_2/Fe^{2+}$) and photo-Fenton-like (e.g., $UV/H_2O_2/Fe^{3+}$) reactions, UV/H_2O_2, UV/TiO_2, microwave decomposition and ionizing radiation treatment [15–18]. More

recently, sulfate radical ($SO_4^{\bullet-}$) based AOPs have also been gaining researchers' attention in degrading organic contaminants [19]. Both $^{\bullet}OH$ and $SO_4^{\bullet-}$ have high redox potentials of 2.72 V [20] and 2.5–3.1 V [21], respectively, depending on the measurement conditions, and therefore, readily attack organic contaminants including endosulfan having a comparable reported second-order rate constant of $1.83 \times 10^9\,M^{-1}\,s^{-1}$ with $^{\bullet}OH$ and $1.50 \times 10^9\,M^{-1}\,s^{-1}$ with $SO_4^{\bullet-}$ [22]. Hydrogen peroxide (H_2O_2), peroxymonosulfate (PMS, HSO_5^-), and persulfate (PS, $S_2O_8^{2-}$) are capable of generating $^{\bullet}OH$ and/or $SO_4^{\bullet-}$ after activation, such as by UV irradiation and transition metals [19,23–25]. Iron (Fe), on the other hand, is naturally abundant, cheap and non-toxic, and consequently has been widely investigated for the catalytic decomposition of peroxides and subsequently the enhancement in the degradation of organic pollutants in water [25–27].

In this study, Fe^{3+} or Fe^{2+} was combined with germicidal UV-254 nm and the dual activation of peroxide by iron and UV was further investigated for the degradation of endosulfan. To minimize the reagent cost while establishing environmentally friendly and economical treatment methods, low concentrations of iron and peroxide were used. A kinetic study on the degradation of endosulfan was assessed by varying initial concentrations of the oxidant, iron, or the target contaminant. Mineralization of endosulfan was elucidated by the UV/peroxide/Fe^{2+} process. Major transformation by-products were also investigated.

2. Materials and methods

2.1. Chemicals and reagents

All the chemicals used in the present study were of high purity and used as received. Standard endosulfan ($C_9H_6Cl_6O_3S$, 406.9 g/mole, 99.5%) and endosulfan ether ($C_9H_6Cl_6O$, 342.86 g/mole, 99.5%) were obtained from Supelco (Bellefonte, PA, USA). Sodium persulfate and potassium peroxymonosulfate (active component of a potassium triple salt, commonly known as Oxone®, $2KHSO_5\cdot KHSO_4\cdot K_2SO_4$) were obtained from Sigma–Aldrich (St. Louis, MO, USA). Hydrogen peroxide (50%, v/v), ferrous sulfate, ferric chloride, methanol, and hydrochloric acid (37.5%, w/w) were purchased from Fischer Scientific (Pittsburgh, PA, USA).

2.2. Analytical methods

An Agilent 7890 gas chromatography (GC) equipped with an Agilent 5975 mass spectrometric detector (MS) and an HP-5MS (5% phenyl methylsiloxane) capillary column (30 m, i.d., 0.25 μm) was used for the detection of endosulfan and its by-products. Solid phase microextraction (SPME) technique with the fiber made of polydimethylsiloxane (PDMS) and fitted with a manual holder (Supelco) was used for a direct injection of samples into the GC. Spectral measurement of the samples was done using an ion trap operated at 70 eV with a scan mode ranging from m/z 50 to 450. Other instrumentation conditions of the GC–MS method are reported in our previous study [22]. The concentration of endosulfan in the present study was the sum of endosulfan stereoisomers, endosulfan I and endosulfan II. The determination of by-products was performed based on comparison of the spectra of the by-products with those of the standards in the NIST library (USA) installed in the GC–MS [22].

A colorimetric method by UV–vis Spectrophotometer (Hewlett Packard, 8452) was used for the quantification of PMS [28]. A Shimadzu VCSH-ASI TOC analyzer was used for monitoring the total organic carbon (TOC).

2.3. Experimental procedure

The photo-assisted experiment was conducted using a UV photochemical apparatus housing two 15 W low-pressure Hg UV lamps (Cole-Parmer) emitting light primarily at $\lambda_{max} = 254$ nm, with an average UV fluence rate of 0.1 mW/cm^2 in the reaction solution [22,29]. This study was conducted at pH 3.0 if not stated otherwise and the pH was adjusted using 0.1 N HCl. Samples were quenched with methanol prior to analysis by GC–MS. Due to the limit of instrumental analysis, a higher initial concentration of 2.45 μM endosulfan was generally used. Other detailed experimental parameters are shown in the figures and tables shown below. For monitoring the TOC removal, an immediate analysis after each treatment was performed without adding any quenching agent. All the experiments were carried out in triplicate with error bars representing the standard error of the mean.

3. Results and discussion

3.1. Performance of UV/Fe and UV/peroxide/Fe

The degradation of endosulfan was evaluated by three different sets of processes, namely, UV only, UV/Fe (i.e., UV/Fe^{3+} and UV/Fe^{2+}), and UV/peroxide/Fe (i.e., UV/peroxide/Fe^{3+} and UV/peroxide/Fe^{2+}, with the peroxide evaluated to be H_2O_2, PS, or PMS). The UV fluence based pseudo first-order rate constant for each reaction condition was determined and is shown in Table 1. The presence of Fe and UV improved the degradation of endosulfan compared to direct UV photolysis, with the degradation under UV/Fe^{3+} being much faster than UV/Fe^{2+}.

After the excitation of organic molecule by light, both the collision between the excited organic molecule and Fe^{3+} [30] and the transfer of an electron from organic molecule to the center of Fe^{3+} in its complex [31] were reported to be responsible for the destruction of organic compounds. A different mechanism was proposed by De Laat et al. [27] who observed that $Fe(OH)^{2+}$ in acidic aqueous solution of Fe^{3+} is highly photosensitive with a molar extinction coefficient at 254 nm of 1500–$3500\,M^{-1}\,cm^{-1}$.

Table 1
Comparison of different processes in the removal of endosulfan in terms of degradation efficiency (%) (calculated at UV fluence of 360 mJ/cm^2), UV fluence based pseudo first-order degradation rate constant (k_{obs}), and EE/O value. Experimental conditions: [endosulfan]$_0$ = 2.45 μM, [peroxide]$_0$ = 49.0 μM, [Fe^{2+}]$_0$ = [Fe^{3+}]$_0$ = 17.8 μM, pH 3.0.

	Percent degradation (%)	k_{obs} (cm^2/mJ)	UV fluence for one-order removal of endosulfan (mJ/cm^2)	EE/O value (kWh m^{-3}/order)
UV only	19.8	6.18×10^{-4}	3.72×10^3	20.2×10^{-1}
UV/Fe^{2+}	32.0	1.11×10^{-3}	2.07×10^3	11.5×10^{-1}
UV/Fe^{3+}	52.4	2.09×10^{-3}	1.10×10^3	6.24×10^{-1}
UV/H_2O_2/Fe^{3+}	69.4	3.45×10^{-3}	6.67×10^2	3.62×10^{-1}
UV/PS/Fe^{3+}	76.8	4.19×10^{-3}	5.50×10^2	3.01×10^{-1}
UV/PMS/Fe^{3+}	86.0	5.83×10^{-3}	3.95×10^2	2.11×10^{-1}
UV/H_2O_2/Fe^{2+}	91.3	6.82×10^{-3}	3.38×10^2	1.82×10^{-1}
UV/PS/Fe^{2+}	93.1	7.62×10^{-3}	3.02×10^2	1.64×10^{-1}
UV/PMS/Fe^{2+}	99.0	12.1×10^{-3}	1.90×10^2	1.03×10^{-1}

Table 2
Rate constants for the potential elementary reactions in the AOPs under different conditions.

No	Reaction	Rate constants ($M^{-1}s^{-1}$)	Ref.
1	$Fe(HO)^{2+} + h\nu \rightarrow Fe^{2+} + {}^{\bullet}OH$	$\Phi = 0.07$	[51]
2	$Fe^{2+} + H_2O_2 \rightarrow Fe^{3+} + OH^- + {}^{\bullet}OH$	70	[52]
3	$Fe^{3+} + H_2O_2 \rightarrow HO_2{}^{\bullet} + Fe^{2+} + H^+$	0.01–0.02	[33]
4	$Fe^{2+} + HSO_5{}^- \rightarrow Fe^{3+} + SO_4{}^{\bullet-} + OH^-$	3.0×10^4	[36]
5	$Fe^{2+} + HSO_5{}^- \rightarrow Fe^{3+} + SO_4{}^{2-} + {}^{\bullet}OH$		[53]
6	$Fe^{2+} + S_2O_8{}^{2-} \rightarrow Fe^{3+} + SO_4{}^{\bullet-} + SO_4{}^{2-}$	27	[54]
7	$Fe^{3+} + HSO_5{}^- \rightarrow Fe^{2+} + SO_5{}^{\bullet-} + H^+$		[36]
8	$H_2O_2/HO_2{}^- + h\nu \rightarrow 2\ {}^{\bullet}OH$	$\Phi = 1.0$	[55]
9	$HSO_5{}^- + h\nu \rightarrow {}^{\bullet}OH + SO_4{}^{\bullet-}$	$\Phi = 1.04$	[56]
10	$S_2O_8{}^{2-} + h\nu \rightarrow 2\ SO_4{}^{\bullet-}$	$\Phi = 1.8$	[57]
11	${}^{\bullet}OH + {}^{\bullet}OH \rightarrow H_2O_2$	5.5×10^9	[14]
12	$SO_4{}^{\bullet-} + SO_4{}^- \rightarrow S_2O_8{}^{2-}$	4.0×10^8	[26]
13	$Fe^{2+} + {}^{\bullet}OH \rightarrow Fe^{3+} + OH^-$	1.9×10^{10}	[49]
14	$Fe^{2+} + SO_4{}^{\bullet-} \rightarrow Fe^{3+} + SO_4{}^{2-}$	4.6×10^9	[58]
15	${}^{\bullet}OH + H_2O_2 \rightarrow H_2O + HO_2{}^{\bullet}$	2.7×10^7	[26]
16	$HSO_5{}^- + SO_4{}^{\bullet-} \rightarrow SO_5{}^{\bullet-} + SO_4{}^{2-} + H^+$	1×10^5	[26]

$Fe(OH)^{2+}$ could therefore be easily photo-reduced by UV-254 nm to Fe^{2+} and generate subsequently reactive ${}^{\bullet}OH$ as shown by Reaction (1) in Table 2 [17,20,32]. As a result, Xu [17] attributed the decolorization of dye X-3B in Fe^{3+} system under UV or visible light irradiation to the attack of ${}^{\bullet}OH$. On the other hand, according to Balzani and Carassiti [31], Fe^{2+} can be oxidized in acidic aqueous solution by UV-254 nm to Fe^{3+} which subsequently generates ${}^{\bullet}OH$ for the degradation of contaminants [32]. The UV/Fe^{2+} was, however, less effective in producing hydroxyl radical [31], which is in agreement with the higher degradation of endosulfan by UV/Fe^{3+} than by UV/Fe^{2+} as observed in the present study.

Addition of peroxides in UV/Fe^{2+} and UV/Fe^{3+} systems significantly increased the removal of endosulfan with UV/peroxide/Fe^{2+} to be more efficient than UV/peroxide/Fe^{3+} regardless of the peroxide type (Table 1). The peroxides can be dissociated into radical species under the dual activation by Fe and UV as shown by Reactions (2)–(10) (Table 2). The reaction between H_2O_2 and Fe^{2+} is faster and can generate ${}^{\bullet}OH$ (Reaction (2) in Table 2) as compared to relatively less reactive $HO_2{}^{\bullet}$ that is generated by H_2O_2/Fe^{3+} (Reaction (3) in Table 2) [33,34], contributing to the faster degradation of endosulfan. Similarly, the activation of PS and PMS by Fe^{2+} has been reported to generate $SO_4{}^{\bullet-}$ and ${}^{\bullet}OH$ (Reactions (4)–(6) in Table 2) as compared to less reactive radical species, such as $SO_5{}^{\bullet-}$ by Fe^{3+} (Reaction (7) in Table 2) [35]. Besides, the oxidation of peroxide by Fe has been reported to take place via electron transfer mechanism involving the transfer of an electron from Fe^{2+} to peroxide in UV/peroxide/Fe^{2+} which is a faster process than the electron transfer from peroxide to Fe^{3+} due to the favorable redox conditions [23,36]. The regeneration of Fe^{2+} by the photo-reduction of Fe^{3+} under UV irradiation catalyzes the UV/peroxide/Fe^{2+} reaction, as shown by Reaction (1) in Table 2, making it a promising AOP for effective water decontamination.

The removal of endosulfan by UV/peroxide/Fe was affected by the type of peroxide as well. At the same initial peroxide molar concentration, i.e., 49.0 μM, UV/PMS/Fe (UV/PMS/Fe^{3+} or UV/PMS/ Fe^{2+}) was found to be more effective in the removal of endosulfan than with the other two oxidants (H_2O_2 and PS), consistent with previous data obtained by Khan et al. [26] and Rastogi et al. [36]. According to Antoniou et al. [24], the oxidizing property of an oxidant depends upon the energy of the lower unoccupied molecular orbital of the central atom to accommodate an electron. A lower energy allows the oxidant to accept an electron more easily and the oxidizing property can subsequently be greater [24]. Therefore, the energy of the three oxidants in the order of PMS < H_2O_2 < PS [24] suggests an easier electron accepting property of the nonsymmetrical PMS and consequently easier activation by transition metals to generate radicals for water decontamination [23,36,37]. The degradation of endosulfan by UV/peroxide/Fe was more in PS than H_2O_2 which was probably due to the lower O—O bond energy in PS leading to a higher radical quantum yield [22,26,38].

To compare the economic efficiency of these processes, the electrical energy per order of degradation (EE/O, $kWh\,m^{-3}$/order of degradation) as recommended by the International Union of Pure and Applied Chemistry (IUPAC) was used [39]. The EE/O value was calculated following an expression in Eq. (1) [26,40].

$$\frac{EE}{O} = \frac{Pt}{V} \tag{1}$$

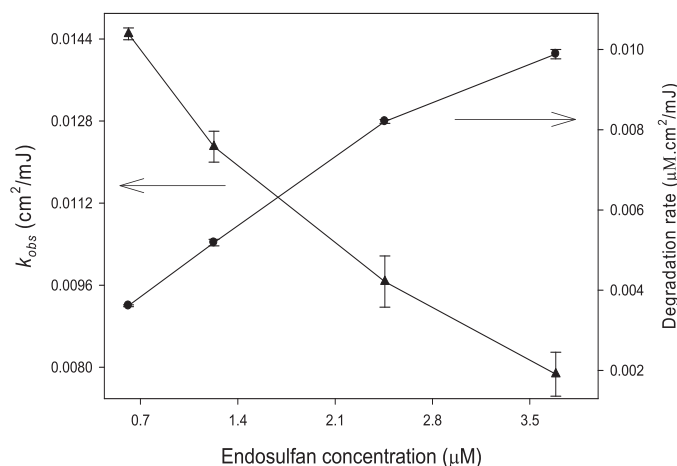where P is the power in kW; t is the exposure time in h and V is the volume of the reaction solution in m^3.

The EE/O results (as shown in Table 1) were found to be in the order: UV/PMS/Fe^{2+} < UV/PS/Fe^{2+} < UV/H_2O_2/Fe^{2+} < UV/PMS/ Fe^{3+} < UV/PS/Fe^{3+} < UV/H_2O_2/Fe^{3+} < UV/Fe^{3+} < UV/Fe^{2+} < UV only, which was in agreement with the above discussion on the degradation efficiency of these iron-mediated AOPs. The most efficient UV/peroxide/Fe^{2+} (i.e., UV/H_2O_2/Fe^{2+}, UV/PS/Fe^{2+} and UV/PMS/Fe^{2+}) processes were further studied and discussed in the following sections.
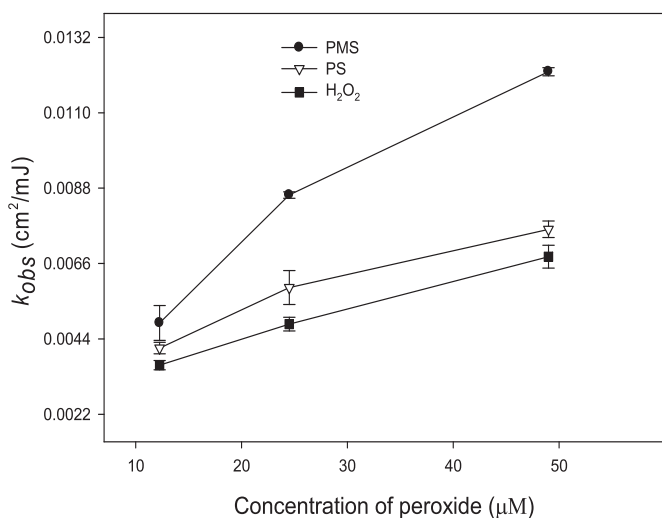
Fig. 1. Variation in UV fluence based pseudo *first-order* degradation rate constant of endosulfan, k_{obs} (cm^2/mJ), at different initial concentrations of peroxide in UV/peroxide/Fe^{2+} processes. Experimental conditions: [endosulfan]$_0$ = 2.45 μM, [peroxide]$_0$ = 12.25, 24.5, and 49.0 μM, [Fe^{2+}]$_0$ = 17.8 μM, pH 3.0.

3.2. Effect of different initial concentrations of peroxide

The peroxide dissociates into reactive radicals (i.e., $^{\bullet}OH$ and/or $SO_4^{\bullet -}$) under the dual activation by UV-254 nm and Fe^{2+} as shown by Reactions (2), (4)–(6), (8)–(10) in Table 2. Elevation of initial concentrations of the peroxide can thus probably result in an increase in the rate of radical formation. As shown in Fig. 1, the degradation of endosulfan was investigated in the present study at different initial peroxide concentrations, i.e., 12.25, 24.5 and 49.0 μM while keeping [Fe^{2+}]$_0$ to be 17.8 μM corresponding to an [oxidant]$_0$/[Fe^{2+}]$_0$ molar ratio of 0.70, 1.40 and 2.75, respectively. Though not including the previously proposed optimum ratio of 1:1 [26], current [oxidant]$_0$/[Fe^{2+}]$_0$ range can still provide useful information on the influence of oxidant dosage on the treatment efficiency. The increased initial concentrations of peroxide led to faster degradation of endosulfan as suggested by the increase in UV fluence based pseudo *first-order* rate constant (k_{obs}, cm^2/mJ). However, the increase in k_{obs} was not linear with increasing [peroxide]$_0$, which was probably due to significant radical scavenging effect of the peroxide as well as the recombination
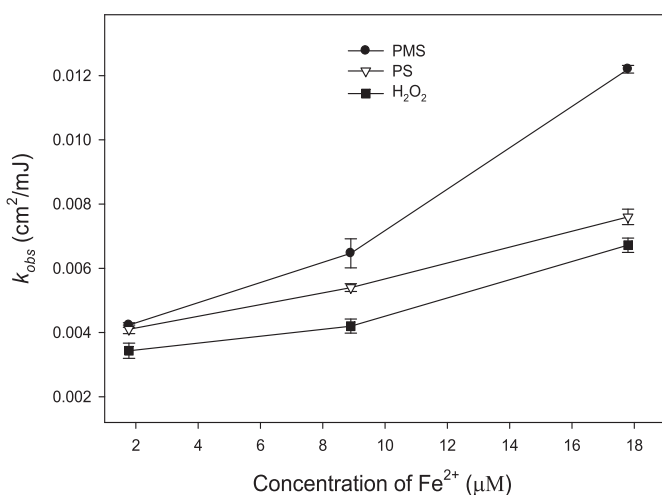
of radical species (Reactions (11)–(16) in Table 2) at high initial peroxide concentrations [34].

3.3. Effect of different initial concentrations of Fe^{2+}

At a high concentration, there can be a problem with Fe^{2+} precipitation, resulting in a complementary secondary treatment and thus higher operational cost for a large-scale water treatment [34]. Lower concentrations of Fe^{2+} were therefore applied in this study. Unlike the effect of [peroxides]$_0$, the k_{obs} of endosulfan degradation was steadily increased with increasing [Fe^{2+}]$_0$ at the current studied reaction conditions as shown in Fig. 2. The rate of radical formation is expected to increase with increasing [Fe^{2+}]$_0$ as shown by Reactions (2), (4)–(6) in Table 2 which in turn, could lead to a faster degradation of endosulfan. The formation of Fe^{3+} as a result of oxidative reactions of Fe^{2+} with $^{\bullet}OH$ and $SO_4^{\bullet -}$ (Reactions (13) and (14) in Table 2) may also contribute to the improved degradation performance, since Fe^{3+}, under UV irradiation (i.e., UV/Fe^{3+}), was highly efficient in the removal of endosulfan as discussed above. Liou et al. [41] reported that the Fe^{2+} promoted efficiency on the degradation rate constant of TNT by photo-Fenton

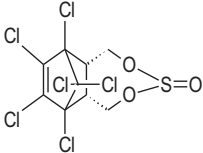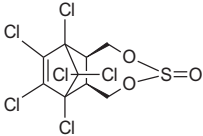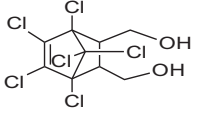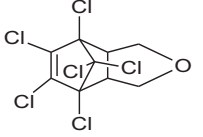**Fig. 3.** Variation in k_{obs} and initial degradation rate (μM cm^2/mJ, calculated from the change in concentration of endosulfan with UV fluence for the initial 120 mJ/cm^2 UV fluence) as a function of different initial concentrations of endosulfan by UV/PMS/Fe^{2+} process. Experimental conditions: [endosulfan]$_0$ = 0.61, 1.22, 2.45, and 3.70 μM, [PMS]$_0$ = 49.0 μM, [Fe^{2+}]$_0$ = 17.8 μM, pH 3.0.
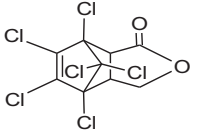

Fig. 2. Variation in k_{obs} at different initial concentrations of Fe^{2+} in UV/peroxide/Fe^{2+} processes. Experimental conditions: [endosulfan]$_0$ = 2.45 μM, [peroxide]$_0$ = 49.0 μM, [Fe^{2+}]$_0$ = 1.78, 8.90, and 17.8 μM, pH 3.0.
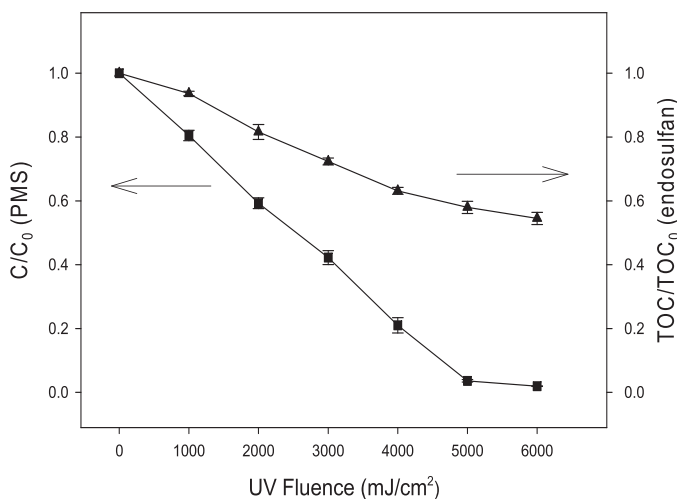
Fig. 4. Removal of TOC and change in PMS residuals in UV/PMS/Fe^{2+} process. Experimental conditions: [endosulfan]$_0$ = 9.80 μM, [PMS]$_0$ = 980 μM, [Fe^{2+}]$_0$ = 17.8 μM, pH 3.0.

Table 3
List of by-products formed during the degradation of endosulfan by the UV/Fe and UV/peroxide/Fe AOPs.

Compound	RT (min)	MW	Structural formula	Detected in process	
				UV/peroxide/Fe	UV only, UV/Fe
Endosulfan I	14.1	406.9			
Endosulfan II	15.8	406.9			
(1) Endosulfan Alcohol	11.3	360.0		√	
(2) Endosulfan Ether	11.2	342.0		√	√
(3) Endosulfan Lactone	15.7	356.0		√	

reaction increased with the increase in Fe^{2+} concentration upto 2.88 mM. This value is much higher than the highest concentration of Fe^{2+}, i.e., 17.8 μM(in the present study), and therefore no inhibition effect of Fe^{2+} was observed herein. Further study is needed to investigate the positive impact of the increase in initial concentration of Fe^{2+} on the k_{obs} of endosulfan degradation.

3.4. Effect of different initial concentrations of endosulfan

The impact of initial concentration of endosulfan was assessed on its degradation by UV/PMS/Fe^{2+} (the most efficient process currently studied) while keeping the initial molar concentrations of Fe^{2+} and PMS constant. At each studied concentration, the initial degradation rate of endosulfan (μM·cm²/mJ) was calculated for the initial 120 mJ/cm² UV fluence. Fig. 3 shows that the initial degradation rate increased from 0.0036 to 0.0099 μM·cm²/mJ when the initial concentration of endosulfan increased from 0.61 to 3.70 μM. Most likely, a larger number of target molecules were exposed to radicals at a higher analyte concentration and consequently resulted in a high degradation rate [26]. However, the increase in [endosulfan]$_0$ decreased the observed degradation rate constant of endosulfan as suggested by k_{obs}. This observation was consistent with the trend observed in previous studies by Devi et al. [42] and Samet et al. [43]. Such decrease in k_{obs} has been attributed to the decrease in the ratio of reactive radicals to the

target contaminant [42]. Besides, the high molar absorption coefficient for endosulfan at 254 nm, $\varepsilon_{254} = 40,877\,M^{-1}\,cm^{-1}$ [22], probably contributed to the strong decrease in the permeability of solution for light absorption when increasing initial concentrations of endosulfan, which affected not only its direct photolysis, but also the activation of PMS for radical generation [44]. Moreover, competition between endosulfan and its by-products for reactive radicals became stronger and thus the apparent degradation rate constant decreased with the elevated initial concentrations of endosulfan [45].
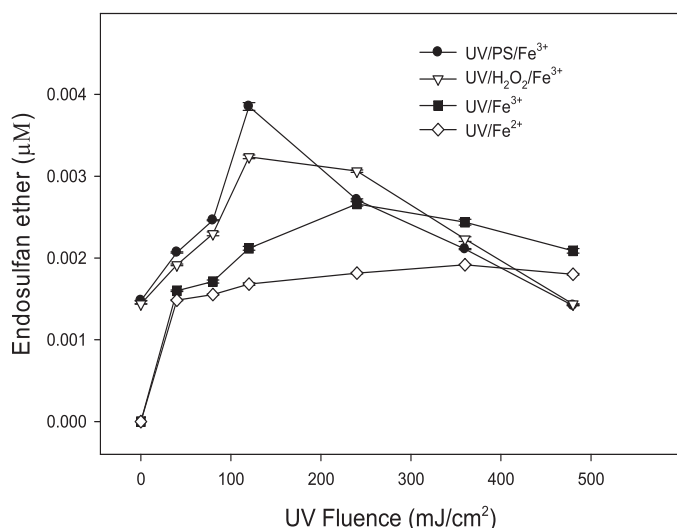
3.5. Mineralization

The study on mineralization indicates a potential decrease in mass concentration of organic pollutant in water bodies and is useful to compare the efficiency of the tested technologies for the removal of target organic contaminants [26,46]. The mineralization of endosulfan was monitored in terms of TOC by UV/PMS/Fe^{2+} process. An [endosulfan]$_0$/[PMS]$_0$ stoichiometric molar ratio of 1:18 for a complete oxidation of endosulfan was estimated by the following stoichiometric reaction (Eq. (2)).

$$C_9H_6Cl_6O_3S + 18HSO_5^- + H_2O \rightarrow 9CO_2 + 6Cl^- + 26H^+ + 19SO_4^{2-} \quad (2)$$
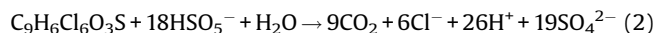
Using UV fluence of 480 mJ/cm², at a given [endosulfan]$_0$/[PMS]$_0$ molar ratio, endosulfan was efficiently removed as

Fig. 5. Change in the concentration of endosulfan ether (μM) as a function of UV fluence by UV/Fe and UV/peroxide/Fe. Experimental conditions: [endosulfan]$_0$ = 2.45 μM, [peroxide]$_0$ = 49.0 μM, [Fe^{2+}]$_0$ = [Fe^{3+}]$_0$ = 17.8 μM, pH 3.0.

discussed earlier in Section 3.1, however, no mineralization of endosulfan in terms of TOC removal was observed. This is possibly due to the fact that mineralization is a complex and multistep process and requires high UV fluence [26,47]. At molar concentrations of 980 μM PMS, 17.8 μM Fe^{2+} and 9.80 μM endosulfan, only 45% of TOC removal was observed at UV fluence as high as 6000 mJ/cm^2 (Fig. 4). The concentration of PMS was also monitored and a rapid decay was shown during the reaction. At UV fluence of 6000 mJ/cm^2, 98% of the PMS was decomposed (Fig. 4). Therefore, the mineralization was relatively fast at the beginning of reaction and slowed down after UV fluence of 4000 mJ/cm^2, which was consistent with the trend observed in previous studies by Khan et al. [26] and Wang and Chu [35].

3.6. Identification of by-products and degradation pathways of endosulfan

The degradation of endosulfan by UV only, UV/Fe and UV/peroxide/Fe resulted in the formation of several by-products. Total of three by-products, i.e., endosulfan alcohol, endosulfan ether and endosulfan lactone, were identified and are shown in Table 3. In UV only and UV/Fe processes, only endosulfan ether was identified; while in UV/peroxide/Fe systems regardless of the peroxide or catalyst type, all the mentioned by-products were detected. The conversion of endosulfan into its corresponding alcohol, ether, and lactone by-products by the attack of hydroxyl and/or sulfate radicals in UV/peroxide/Fe processes was probably through hydrogen abstraction and/or electron transfer mechanisms, which have been explained in detail in our previous publication [22].

Endosulfan ether was the most significant by-product. The GC–MS analysis showed two isomeric forms of endosulfan, identified by the mass spectral search program (NIST, USA) installed in the GC–MS as endosulfan I (retention time (RT) = 14.1 min) and endosulfan II (RT = 15.8 min). However, the by-products were detected at only one single RT. The seven membered dioxathiepine-3-oxide ring in endosulfan contains a sulfite group, this sulfite group undergoes conformational and configurational changes due to attractive interaction between the lone pair of electrons on sulfur and the axial hydrogen on the adjacent methylene groups [48]. As a result, two conformational isomers of endosulfan are formed. The loss of the sulfur moiety due to the

attack of radical species may therefore lead to the detection of aforementioned three by-products with only one isomeric form. In fact, the study by Forman et al. [48] also showed that isomerism in endosulfan arose due to pyramidal stereochemistry of sulfite group and both endosulfan isomers yielded identical endosulfan alcohol, endosulfan ether, and endosulfan lactone.

Fig. 5 illustrates variation in endosulfan ether treated by UV/Fe^{3+}, UV/Fe^{2+}, UV/H$_2$O$_2$/Fe^{3+} and UV/PS/Fe^{3+}. It was also observed in UV/PMS/Fe^{3+} and UV/peroxide/Fe^{2+} processes, but the concentration was not high enough to be quantified possibly due to their high treatment efficiency. The formation and further destruction of endosulfan ether by different processes was consistent with the effectiveness of these processes in degrading parent endosulfan as discussed above. It shows again the effectiveness of iron-mediated AOPs for water decontamination.

The presented by-product identification, elucidation of degradation pathways and mineralization provide important fundamental literature information on the removal and potentially toxicity reduction of endosulfan. The formed main by-products (alcohol, ether and lactone) have been reported to be non-toxic suggesting a successful detoxification of endosulfan [12]. It has been interpreted by Shah et al. [49] and Khan et al. [50] that the chlorine group was mainly responsible for the toxicity of organochlorine compounds and their by-products. The mineralization of endosulfan as estimated by stoichiometric reaction (Eq. (2)) indicated a significant loss of chloride ion by the tested technologies, suggesting the decrease in the toxicity of the target contaminant. Nevertheless, more studies are required to evaluate the toxicity of the by-products of endosulfan.

4. Conclusions

Three different UV based processes were investigated for the degradation of endosulfan, i.e., UV only, UV/Fe and UV/peroxide/Fe. The main pathway of endosulfan degradation was most likely from the reaction of $^{\bullet}$OH and/or SO$_4^{\bullet-}$ generated. Iron can be activated by UV, promoting the removal of endosulfan as compared to UV only process. Dual activation of peroxide by UV and iron was found to be more efficient. The observed degradation rate constant of endosulfan increased significantly with increasing initial concentrations of peroxide or Fe^{2+} at the present studied conditions. The TOC reduction was a slow process by UV/PMS/Fe^{2+} especially at the later stage of irradiation treatment when most of PMS was decomposed. The formation and further disappearance of endosulfan ether as a function of different UV fluence suggested that iron-mediated AOPs are good alternative technologies for the removal of endosulfan and its by-products from contaminated water. This study is useful for the potential practical applications of AOPs in the presence of natural transition metals for environmental remediation.

References

[1] A.H. Arias, T.P. Marcelo, E.M. Jorge, Multi-year monitoring of estuarine sediments as ultimate sink for DDT, HCH and other organochlorinated pesticides in Argentina, Environ. Monit. Assess. 172 (2011) 17–32.

[2] S.A. Tiyagi, S. Ajaz, M.F. Azam, Effect of some pesticides on plant growth root nodulation and chlorophyll content of chickpea, Arch. Agron. Soil Sci. 50 (2004) 529–533.

[3] X.-M. Xie, M. Liao, C.-Y. Huang, W.-P. Liu, S. Abid, Effects of pesticides on soil biochemical characteristics of a paddy soil, J. Environ. Sci. 16 (2004) 252–255.

[4] H.S. Sandhu, R.S. Brar, Pesticides, Textbook of Veterinary Toxicology, Kalyani Publishers, Ludhiana, New Delhi, India, 2009.

[5] U. Tiemann, In vivo and in vitro effects of the organochlorine pesticides DDT, TCPM, methoxychlor and lindane on the female reproductive tract of mammals: a review, Reprod. Toxicol. 25 (2008) 316–326.

[6] C.P. Rice, S.M. Chernyak, C.J. Hapeman, S. Bilboulian, Air–water distribution of the endosulfan isomers, J. Environ. Qual. 26 (1997) 1101–1107.

[7] G.F. Antonius, M.E. Byers, J.C. Snyder, Residues and fate of endosulfan on field-grown pepper and tomato, Pest. Sci. 54 (1998) 61–67.

[8] Y. Lu, K. Morimoto, T. Takeshita, T. Takeuchi, T. Saito, Genotoxic effects of α-endosulfan and β-endosulfan on human HepG2 cells, Environ. Health Perspect. 108 (2000) 559–561.

[9] S.B. Chattopadhyay, Principles and Procedures of Plant Protection, Oxford and IBH publishing Co. Pvt. Ltd., New Delhi, India, 1993, pp. 85–86.

[10] USEPA, office of prevention pesticides, Endosulfan Red Facts, US Environmental Protection Agency, Washington DC, USA, 2002.

[11] A. Kaushik, H.R. Sharma, S. Jain, S. Dawra, C.P. Kaushik, Pesticide pollution of river Ghaggar in Haryana, India, Environ. Monit. Assess. 160 (2010) 61–69.

[12] N.S. Shah, J.A. Khan, S. Nawaz, H.M. Khan, Role of aqueous electron and hydroxyl radical in the removal of endosulfan from aqueous solution using gamma irradiation, J. Hazard. Mater. 278 (2014) 40–48.

[13] D.J. Hamilton, A. Ambrus, R.M. Dieterle, A.S. Felsot, C.A. Harris, P.T. Holland, A. Katayama, N. Kurihara, J. Linders, J. Unsworth, S.S. Wong, Regulatory limits for pesticide residues in water (IUPAC Technical report), Pure Appl. Chem. 75 (2003) 1123–1155.

[14] G.V. Buxton, C.L. Greenstock, W.P. Helman, A.B. Rose, Critical review of rate constants for reactions of hydrated electrons, hydrogen atoms and hydroxyl radicals ($^•OH/O^{•-}$) in aqueous solution, J. Phys. Chem. Ref. Data 17 (1988) 513–780.

[15] S. Chiron, A. Fernandez-Alba, A. Rodriquez, E. Garcia-Calvo, Pesticide chemical oxidation: state-of-the-art, Water Res. 34 (2000) 366–377.

[16] J.A. Herrera-Melian, E. Tello Rendon, J.M. Dona Rodriguez, A. Viera Suarez, C. Valdes Do Campo, J. Perez Pena, J. Arana Mesa, Incidence of pretreatment by potassium permanganate on hazardous laboratory wastes photodegradability, Water Res. 34 (2000) 3967–3976.

[17] Y. Xu, Comparative studies of the $Fe^{3+}/^{2+}$-UV, H_2O_2-UV TiO_2-UV/vis systems for the decolorization of a textile dye X-3B in water, Chemosphere 43 (2001) 1103–1107.

[18] M. Trapido, I. Epold, J. Bolobajev, N. Dulova, Emerging micropollutants in water/wastewater: growing demand on removal technologies, Environ. Sci. Pollut. Res. (2014) 1–6.

[19] S. Yang, P. Wang, X. Yang, L. Shan, W. Zhang, X. Shao, R. Niu, Degradation efficiencies of azo dye Acid Orange 7 by the interaction of heat, UV and anions with common oxidants: persulfate, peroxymonosulfate and hydrogen peroxide, J. Hazard. Mater. 179 (2010) 552–558.

[20] D.M. Stanbury, A.G. Sykes, Advances in Inorganic Chemistry, 33, Academic Press, New York, 1989, pp. 69.

[21] P. Neta, R.E. Huie, A.B. Ross, Rate constants for reactions of inorganic radicals in aqueous solution, J. Phys. Chem. Ref. Data 17 (1988) 1027–1284.

[22] N.S. Shah, X. He, H.M. Khan, J.A. Khan, K.E. O'Shea, D.L. Boccelli, D.D. Dionysiou, Efficient removal of endosulfan from aqueous solution by UV-C/peroxides: a comparative study, J. Hazard. Mater. 263 (2013) 584–592.

[23] G.P. Anipsitakis, D.D. Dionysiou, Radical generation by the interaction of transition metals with common oxidants, Environ. Sci. Technol. 38 (2004) 3705–3712.

[24] M.G. Antoniou, A.A. de la Cruz, D.D. Dionysiou, Degradation of microcystin-LR using sulfate radicals generated through photolysis, thermolysis and e^- transfer mechanisms, Appl. Catal. B: Environ. 96 (2010) 290–298.

[25] P. Nfodzo, H. Choi, Triclosan decomposition by sulfate radicals: effects of oxidants and metal ions, Chem. Eng. J. 174 (2011) 629–634.

[26] J.A. Khan, X. He, H.M. Khan, N.S. Shah, D.D. Dionysiou, Oxidative degradation of atrazine in aqueous solution by $UV/H_2O_2/Fe^{2+}$, $UV/S_2O_8^{2-}/Fe^{2+}$ and $UV/HSO_5^-/Fe^{2+}$ processes: a comparative study, Chem. Eng. J. 218 (2013) 376–383.

[27] J. De Laat, H. Gallard, S. Ancelin, B. Legube, Comparative study of the oxidation of atrazine and acetone by H_2O_2/UV, $Fe(III)/UV$ $Fe(III)/H_2O_2/UV$ and $Fe(II)$ or $Fe(III)/H_2O_2$, Chemosphere 39 (1999) 2693–2706.

[28] C. Liang, C.-F. Huang, N. Mohanty, R.M. Kurakalva, A rapid spectrophotometric determination of persulfate anion in ISCO, Chemosphere 73 (2008) 1540–1543.

[29] X. He, A.A. de la Cruz, D.D. Dionysiou, Destruction of cyanobacterial toxin cylindrospermopsin by hydroxyl radicals and sulfate radicals using UV-254 nm activation of hydrogen peroxide, persulfate and peroxymonosulfate, J. Photochem. Photobiol. A Chem. 251 (2013) 160–166.

[30] K. Wu, Photo-Fenton degradation of a dye under visible light irradiation, J. Mol. Catal. A: Chem. 144 (1999) 77–85.

[31] V. Balzani, V. Carassiti, Photochemistry of Coordination Compounds, Academic Press, New York, USA, 1970, pp. 159.

[32] I.P. Pozdnyakov, E.M. Glebov, V.F. Plyusnin, V.P. Grivin, Y.V. Ivanov, D.Y. Vorobyev, N.M. Bazhin, Mechanism of $Fe(OH)^{2+}_{(aq)}$ photolysis in aqueous solution, Pure Appl. Chem. 72 (2000) 2187–2197.

[33] A. Mehrdad, B. Massoumi, R. Hashemzadeh, Kinetic study of degradation of Rhodamine B in the presence of hydrogen peroxide and some metal oxide, Chem. Eng. J. 168 (2011) 1073–1078.

[34] E. Evgenidou, I. Konstantinou, K. Fytianos, I. Poulios, Oxidation of two organophosphorous insecticides by the photo-assisted Fenton reaction, Water Res. 41 (2007) 2015–2027.

[35] Y.R. Wang, W. Chu, Degradation of a xanthene dye by Fe(II)-mediated activation of Oxone process, J. Hazard. Mater. 186 (2011) 1455–1461.

[36] A. Rastogi, S.R. Al-Abed, D.D. Dionysiou, Sulfate radical-based ferrous peroxymonosulfate oxidative system for PCBs degradation in aqueous and sediment systems, Appl. Catal. B: Environ. 85 (2009) 171–179.

[37] B. Meunier, Potassium monopersulfate – just another primary oxidant or a highly versatile oxygen atom donor in metalloporphyrin-mediated oxygenation and oxidation reactions, New J. Chem. 16 (1992) 203–211.

[38] J.A. Khan, X. He, N.S. Shah, H.M. Khan, E. Hapeshi, D. Fatta-Kassinos, D.D. Dionysiou, Kinetic and mechanism investigation on the photochemical degradation of atrazine with activated H_2O_2, $S_2O_8^{2-}$ and HSO_5^-, Chem. Eng. J. 252 (2014) 393–403.

[39] J.R. Bolton, Ultraviolet Applications Handbook, 2nd ed., Bolton Photosciences Inc., 2001, pp. 27.

[40] J.R. Bolton, K.G. Bircher, W. Tumas, C.A. Tolman, Figures-of-merit for the technical development and application of advanced oxidation processes, J. Adv. Oxid. Technol. 1 (1996) 13–17.

[41] M.-J. Liou, M.-C. Lu, J.-N. Chen, Oxidation of TNT by photo-Fenton process, Chemosphere 57 (2004) 1107–1114.

[42] L.G. Devi, K.S.A. Raju, S.G. Kumar, K.E. Rajashekhar, Photo-degradation of di azo dye Bismarck Brown by advanced photo-Fenton process: influence of inorganic anions and evaluation of recycling efficiency of iron powder, J. Taiwan Inst. Chem. Eng. 42 (2011) 341–349.

[43] Y. Samet, I. Wali, R. Abdelhédi, Kinetic degradation of the pollutant guaiacol by dark Fenton and solar photo-Fenton processes, Environ. Sci. Pollut. Res. 18 (2011) 1497–1507.

[44] K. Dutta, S. Mukhopadhyay, S. Bhattacharjee, B. Chaudhuri, Chemical oxidation of methylene blue using a Fenton-like reaction, J. Hazard. Mater. 84 (2001) 57–71.

[45] H. Ghodbane, O. Hamdaoui, Decolorization of antraquinonic dye, C.I. Acid Blue 25, in aqueous solution by direct UV irradiation, UV/H_2O_2 and UV/Fe(II) processes, Chem. Eng J 160 (2010) 226–231.

[46] Y. Shi, L. Xu, D. Gong, J. Lu, Effects of sterilization treatments on the analysis of TOC in water samples, J. Environ. Sci. 22 (2010) 789–795.

[47] A. Riga, K. Soutsas, K. Ntampegliotis, V. Karyannis, G. Papapolymerou, Effect of system parameters and of inorganic salts on the decolorization and degradation of Procion H-exl dyes. Comparison of H_2O_2/UV, Fenton, UV/Fenton, TiO_2/UV and $TiO_2/UV/H_2O_2$ processes, Desalination 211 (2007) 72–86.

[48] S.E. Forman, A.J. Durbetaki, M.V. Cohen, R.A. Olofson, Conformational equilibria in cyclic sulfites and sulfates. The configurations and conformations of the two isomeric thiodans[1], J. Org. Chem. 30 (1965) 169–175.

[49] N.S. Shah, J.A. Khan, S. Nawaz, M. Ismail, K. Khan, H.M. Khan, Kinetic and mechanism investigation on the gamma irradiation induced degradation of endosulfan sulfate, Chemosphere 121 (2015) 18–25.

[50] J.A. Khan, N.S. Shah, S. Nawaz, M. Ismail, F. Rehman, H.M. Khan, Role of e^-_{aq}, $^•OH$ and $H^•$ in radiolytic degradation of atrazine: a kinetic and mechanistic approach, J. Hazard. Mater. 288 (2015) 147–157.

[51] R. Chen, J.J. Pignatello, Role of quinone intermediates as electron shuttles in Fenton and photoassisted Fenton oxidations of aromatic compounds, Environ. Sci. Technol. 31 (1997) 2399–2406.

[52] E. Neyens, J. Baeyens, A review of classic Fenton's peroxidation as an advanced oxidation technique, J. Hazard. Mater. 98 (2003) 33–50.

[53] P. Neta, R.E. Huie, Free-radical chemistry of sulfite, Environ. Health Perspect. 64 (1985) 209–217.

[54] L.R. Bennedsen, J. Muff, E.G. Søgaardet, Influence of chloride and carbonates on the reactivity of activated persulfate, Chemosphere 86 (2012) 1092–1097.

[55] J.H. Baxendale, J.A. Wilson, The photolysis of hydrogen peroxide at high light intensities, Trans. Faraday Soc. 53 (1957) 344–356.

[56] G. Mark, M.N. Schuchmann, H.-P. Schuchmann, C. von Sonntag, The photolysis of potassium peroxodisulphate in aqueous solution in the presence of tertbutanol: a simple actinometer for 254 nm radiation, J. Photochem. Photobiol. A: Chem. 55 (1990) 157–168.

[57] Y. Guan, J. Ma, X. Li, J. Fang, L. Chen, Influence of pH on the formation of sulfate and hydroxyl radicals in the UV/peroxymonosulfate system, Environ. Sci. Technol. 45 (2011) 9308–9314.

[58] G.V. Buxton, T.N. Malone, G. Arthur Salmon, Reaction of SO_4^- with Fe^{2+}, Mn^{2+} and Cu^{2+} in aqueous solution, J. Chem. Soc. Faraday Trans. 93 (1997) 2893–2897.